Frontiers in Mechanochemistry and Mechanical Alloying

INCOME2008
1-4 December, 2008

CHANGES IN THE STRUCTURE OF TALC BY CONTINUOUS JET MILLING IN RELATION TO IMPOSED SPECIFIC KINETIC ENERGY

Samayamutthirian Palaniandy[ξ], Khairun Azizi Mohd Azizli, Hashim Hussin, Syed Fuad Saiyid Hashim
School of Materials and Mineral Resources Engineering, Engineering Campus,
Universiti Sains Malaysia, 14300 Nibong Tebal, Penang, Malaysia

Keywords: Jet mill, Talc, Mechanochemical, Specific kinetic energy

Abstract

Ultra fine talc is used in many industries such as paper, paints, polymers, cosmetics and pharmaceutical. Emerging demand with stringent specification from these industries has marked jet mill as one of the essential grinding mill to produce ultra fine talc. Ultra fine grinding testwork of talc was carried out in opposed fluidized bed jet mill by varying the feed rate, classifier rotational speed and grinding pressure at three levels. In this jet mill, grinding and classification took place simultaneously. The ground products were characterized in terms of particle size distribution and mechanochemical effect via X-ray diffraction. The ground product exhibited poly-modal distribution and the minimum size obtained was 4.28 µm at 4 kg/h, 13000 rpm and 4 bar. Besides size reduction in micron range, mechanochemical effect was exhibited by the product ground in jet mill as jet mill is classified as high-energy mill. Reduction in peak intensity and peak base broadening was observed which indicates fine grinding process in jet mill induced mechanochemical effect. Furthermore preferential distortion of (00*l*) planes was observed as well. The degree of crystallinity of ground sample, which ranged from 26.5% to 85.3% reduces as the specific kinetic energy increase and its reduction gradient varies according to the classifier rotational speed. The crystallite size and lattice strain of talc ranged from 147.69 nm to 353.72 nm and 0.08 to 0.2 respectively.

Introduction

Talc [$Mg_3Si_4O_{10}(OH_2)$] is layer silicate whose structure consists of a sheet of octahedrally coordinated Mg sandwiched between two sheets of tetrahedrally coordinated Si. The structure of talc do not show any residual charges and there are no interlayer cations. The layers are bonded together by weak van de Waals forces. The softness of talc is also due to the ease of displacement of these layers [1]. Talc is widely used in cosmetics, pharmaceutical, paint, paper, pesticides and ceramics. Application of talc with well defined crystallinity, particle size distribution and surface area constitute a promising way for achieving the desired properties. Sanchez-Sato *et al* (1997) and Terada and Yonemochi (2004) have conducted extensive research work on mechanochemical effect of talc in vibration mill and planetary ball mill [1-2]. The structure, particle size and particle shape of talc were modified during fine grinding process [2]. Godet-Morand et. al. (2002) has carried out fine grinding process of talc in jet mill but the testwork were more focused on the optimization of the fine grinding process in jet mill. Limited literature was found for mechanochemical effect of talc ground in jet mill [3].

Fine grinding is an intermediate case between coarse grinding and mechanical activation. Fine grinding is normally carried out in high intensity grinding mills such as oscillating mill, planetary mill, vibration mill, attrition mill and jet mill. Jet mills are commonly used to produce particle sizes between 1µm to 10µm and it is widely used in the chemical, pharmaceutical and mineral industries [4-6]. Jet mills exhibit various advantages such as the ability to produce micron-sized particles with narrow size distribution, absence of contamination caused by autogenous grinding, low wear rate, low noise, small footprint and ability to grind heat sensitive materials [6-7]. The disadvantage of jet mill is its high-energy consumption where only 2% of the energy supplied is used for particle breakage [8]. Besides size reduction, severe and intense mechanical action on the solid surface during fine grinding process are known to lead to physical and chemical changes in the near-surface region where solids come into contact under mechanical forces due to the huge amount of energy delivered by the grinding mills. The mechanically initiated physicochemical effects in particles are generally termed as mechanochemical effect [9].

Mechanochemical effect is evident in solids when they are ground with equipment based on impact and shear among the particles [10]. Due to low thermal conductivity characteristics of most of nonmetallic solids, the energy delivered by the mill is not stored in the particle as thermal energy, but applied to the bending and/or breaking of crystal lattice. This treatment brings about loss of crystallinity (amorphisation) as well as formation of active surfaces and leads to increase to reactivity [10-11]. Deformation result from the relative slip of crystal following either edge or screw dislocation, or a dislocation with edge and screw component [10]. Dislocation and various structural defects produced in the crystal lattice as a result of mechanochemical effect cause accumulation of energy, where the amount of mechanochemical effect storage energy is 10% - 20% of the total energy supplied during fine grinding process.

Research in mechanochemical effect of minerals has been carried out extensively for the past 20 years as they are many advantages that can be derived from this effect such as reducing the annealing and sintering temperature, surface tension, accelerate the rate of densification in ceramics powder, increase disintegration time and dissolution rate of pharmaceutical products, production of porous minerals, increase the reactivity of cementitious waste materials, reduction in phase transformation temperature, enhance leaching process, decrease thermal decomposition temperature, increase in particle reactivity and in environment [2, 9, 12 -14]. Almost all

[ξ] email : s.palaniandy@uq.edu.au
Present address: JKMRC, University of Queensland, Australia

the testwork was carried out in high-energy bulk density grinding mills such as planetary mill, vibration mill and oscillating mill for longer grinding period [12]. Aglietti *et al*, (1986) has studied on mechanochemical effect of kaolinite in short grinding period and found that preference mechanochemical effect took place at (001) plane as kaolinite was layered structured mineral. Mechanochemical effect does not necessarily takes place during longer grinding period but it also depends on the types of materials and the amount of energy transferred to the particle by the grinding media [11,16]. In the present study, continuous fine grinding of talc was performed in jet mill to investigate the extend of mechanochemical effect in relation with imposed specific kinetic energy.

Experimental

The fine grinding test work was carried out with an Alpine 100 AFG fluidized bed jet mill (hereafter will be referred as jet mill) equipped with a 50mm ATP-forced vortex classifier (hereafter will be referred as classifier). The fine grinding test work was carried out by varying the operational parameters of the jet mill such as feed rate, classifier rotational speed and grinding pressure according to the 3^3 experimental designs as shown in Table 1. The total numbers of experiments were 27. The grinding period was kept constant for 30 minutes and the jet mill was sharply stopped after 30 minutes to collect the samples from the sample collection bin as the jet mill reached the steady state condition within 15 minutes [3]. The talc used in this study was from Lioning China and Table 2 shows the chemical composition of talc used in this test work.

Table 1. Range of operational parameters

Operational parameters	Level		
	Level 1	Level 2	Level 3
Feed rate (kg/h)	4	12	20
Classifier rotational speed (rpm)	7000	13000	20000
Grinding pressure (bar)	2	4	6

Table 2. Chemical composition of silica

Composition	Al_2O_3	SiO_2	MgO	CaO	Fe_2O_3	NiO
Weight, %	0.16	47.0	49.0	3.0	0.45	0.028

The particle size distribution of the feed and ground product was determined by wet laser diffraction using a Malvern Mastersizer 2000s apparatus. The parameters used from the particle size distribution data were volume moment diameter, $d(4.3)$ and the span value. $d(4.3)$ was more preferred compared to the d_{50} value since the particle size distribution had poly-modal distribution as d_{50} did not represent well the particle size distribution of the samples. $d(4.3)$ was calculated by Malvern Mastersizer with x_k number percentage of detected diameter d_k as shown in eq. 1 [17]. The span values, ψ showed the particle size distribution of the samples and it was calculated using eq. 2 from the values obtained from the particle size analysis data where diameter indicating i% smaller than d_i (i = 10%, 50% and 90%) [18].

$$d(4.3) = (\sum x_k d_k^4)/(\sum x_k d_k^3) \quad (1)$$

$$\psi = (d_{90} - d_{10})/2d_{50} \quad (2)$$

The feed had a volume moment diameter, d(4.3) of 18.73µm with a span value of 1.71.Talc was chosen as the raw material for this testwork as has vast application as filler especially when its mean size is below 10µm.

The X-ray diffraction (XRD) patterns were collected using Philips equipment model PW 1140/00. Radiation K_α of Cu (λ = 1.542 Å) was used for all analyses, at 40kV and 20 mA. The XRD pattern samples were recorded in the range $2\theta = 10^0 - 70^0$ using a step size of 0.05^0 and counting time of 5s per step. Silicon powder was used as standard to remove the instrumental broadening effects from the observed profile broadening. Line positions, intensities widths and shapes were obtained from the XRD spectra in order to characterize the microstructure in terms of defects parameter such as crystalline size and microstrain. The APD version 4.1g software was used to obtain these parameters. The $K_{\alpha 2}$ component was removed from the XRD spectra with the assumption that $K_{\alpha 2}$ intensity was half of the $K_{\alpha 1}$ intensity. The (101), (110), (200) and (202) planes were selected for the profile analysis. The overlapped peak was split using the APD version 4.1g software. The X-ray diffraction patterns were adjusted to a combination of Cauchy and Gaussian line shape, using the Halder and Wagner method for obtaining the physical broadening as shown in eq. 3 where β_f, β_h and β_g are the integral breadths of the instrumental, observed and measured profiles respectively. The profile fitting procedure was performed without smoothing the XRD spectra. Each goodness factor was refined to a value of <5% for all the reflection. Maximum height of the peak (I_{max}), integral breath of line profile ($\beta = A/I_{max}$), full-width at half maximum (FWHM) and peak position (2θ) were obtained from the adjusted line profile. A is the area under the peak. The apparent crystallite size was calculated using the Scherrer Equation as shown in eq. 4. The Scherrer formula describes the mutual dependence between the line profile integral breath and crystallite size, D_v which was the volume weighted mean of the crystallite in the direction perpendicular to the diffracting planes; the constant varied with the reflection Bragg angle and crystallite shape. Lattice strain was calculated using eq. 5. The structural disorder due to increasing abundance of X-ray amorphous material was manifested through the reduction in the integral intensity of diffraction lines [19].The relative fractional amorphization (Am) defined in eq. 6 was based on the area under the (002) peak where A_0 and and A is the area under the peak for feed and ground sample respectively [15].

$$\beta_f = (\beta_h^2 - \beta_g^2)/\beta_h \quad (3)$$

Where β_f, β_h and β_g are the integral breadths of the instrumental, observed and measured profiles respectively (Pourghahramani and Forssberg, 2006 [19]).

$$D_v = (K\lambda/FWHM)\cos\theta \quad (4)$$

where D_v is volume weighted mean of the crystallite size, K is the constant, θ is the Bragg angle of (h k l) reflection and λ is the wavelength of X-rays used [19].

$$\varepsilon = \beta / 4\tan\theta \quad (5)$$

where ε is lattice strain (Pourghahramani and Forssberg, 2006).

$$Am = ((A_0 - A_t)/A_0) \times 100 \quad (6)$$

where Am is fractional amorphization. A_0 and and A_t are the area under the peak for feed and ground sample respectively (Benezet and Benhassaine, 1999).

The specific kinetic energy in the jet mill was influenced by the grinding pressure and feed rate. The kinetic energy was calculated using eq. 7.

$$E_{Kinetic} = 0.5 m_g v^2 \quad (7)$$

where $E_{kinetic}$ was kinetic energy, m_g was mass of gas and v is gas velocity.

The Bernoulli Equation as shown in eq. 8 calculated the gas velocity.

$$v = \varphi\sqrt{2P/\rho_g} \quad (8)$$

where φ was gas constant, P was gas pressure and ρ_g was gas density.
The specific energy consumption was calculated using Eq. 9.

$$SEC = E_{kinetic} / F \quad (9)$$

where SEC was specific energy consumption and F is feed rate.

Results and Discussion

Jet mill had the ability to produce particles below 10μm with narrow size distribution. The jet mill also induced mechanochemical effect besides particle size reduction due to the huge amount of energy delivered to the mill. Therefore, it was essential to optimize the jet mill in terms of energy consumption to obtain optimum particle breakage without jeopardizing the product quality. Specific kinetic energy was used to quantify the energy usage for particle breakage.

The specific kinetic energy in the jet mill was dependent on the grinding pressure and feed rate [17]. Operational parameters that were considered in the specific energy consumption calculation were the mass flow rate of the grinding fluids, the velocity of the grinding fluids and feed rate. In order to determine the specific kinetic energy in terms of product fineness, d(4.3) was plotted against various specific kinetic energy as shown in Fig. 1. Generally the d(4.3) decreased as the specific energy consumption increased for but there was a transition value for the specific energy consumption 1000 kWh/ton for talc. The specific energy consumption below 1000 kWh/ton exhibited sharp decreased in the d(4.3) values, and above 1000 kWh/ton the d(4.3) values increased. Above 1000 kWh/ton of energy input, the d(4.3) values increased showing that any increased in specific kinetic energy would resulted in coarser particles. This phenomenon may be due to creation of highly active surface which resulted in agglomeration of finely ground particles.

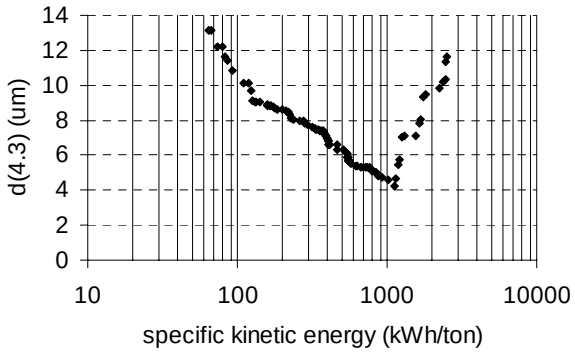

Figure 1. d(4.3) of talc at various levels of specific kinetic energy

Figure 2 shows the agglomerated particles ground when 1766.4 kWh/ton. In this jet mill there were many factors influencing the grinding process such as classification within the grinding chamber, holdup behavior and grinding chamber pressure. Slightly under pressure condition in the grinding chamber and sufficient holdup amount, around 250g were essential parameters to obtain optimum product fineness. Higher grinding pressure led to higher grinding chamber pressure, which resulted in classification of coarser particles due to high drag force. These possible factors produced coarser particles at high specific kinetic energy besides particle agglomeration.

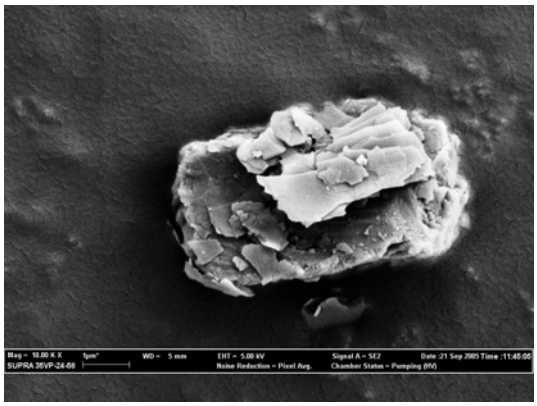

Figure 2. Micrograph of talc ground at 1766.4 kWh/tonne

Besides particle size, the behavior of particle size distribution was studied as well. Figure 3 shows the span values at various specific energy consumption of talc. Figure 3 shows the span value of talc decreased as the specific kinetic energy increased. When the specific kinetic energy was low, the breakage of the particle took place along the weak planes which resulted in platy particles. As the specific kinetic energy increased, destructive breakage mechanism became dominant and due to softness of talc, it was forced to break in random direction. Figure 3 shows that talc exhibited wider particle size distribution when it was ground at lower grinding pressure and higher feed rate whilst narrow size distribution was obtained when talc was ground at higher grinding pressure and lower feed rate. This phenomenon indicated the reason of obtaining high span values at lower specific kinetic energy.

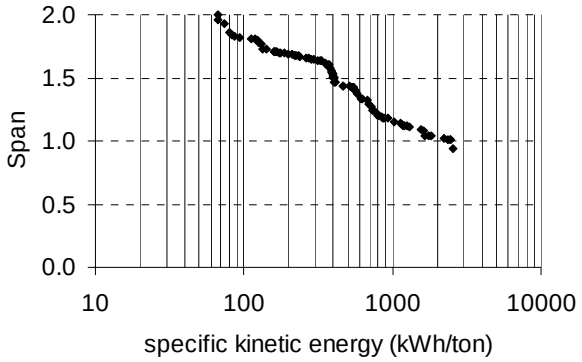

Figure 3. Span values of talc at various levels of specific kinetic energy

Figure 4 shows the degree of crystallinity of talc at various levels of specific kinetic energy. The degree of crystallinity of talc decreased as the specific kinetic energy increased. Theoretically, as the specific kinetic energy increased, the degree of crystallinity decreased but the mechanochemical process in jet mill was accompanied by continuous classification. The classification factor was not included in the calculation for specific kinetic energy. At higher classifier rotational speed, the retention time of the particles in the grinding chamber was short which led to classification of crystalline particles. Talc exhibited reduction in degree of crystallinity as the specific kinetic energy increased. Although classification played an important role in the comminution process in jet mill, but the softness of talc played an important factor as well.

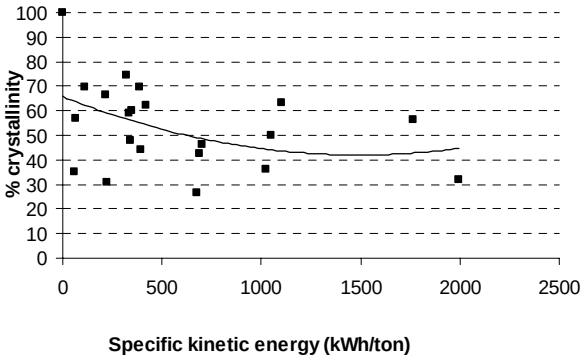

Figure 4: Degree of crystallinity of talc at various level of specific kinetic energy

Figures 5 and 6 show the crystallite size and lattice strain at various levels of specific kinetic energy. The crystallite size ranged from 188.9 nm to 342.67 nm whilst the lattice strain ranged from 0.08% to 0.15%. Minimum crystallite of 188.9 nm was obtained at 1024 kWh/ton. The trend of crystallite size and lattice strain is accordingly with degree of crystallinity.

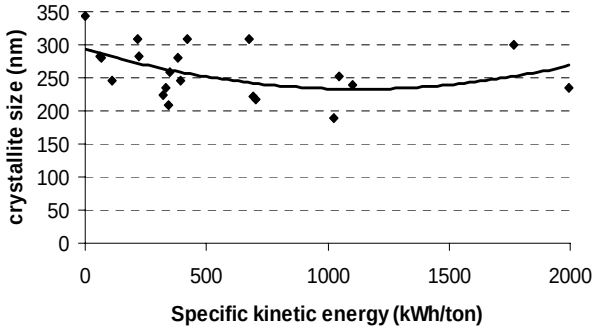

Figure 5. Crystallite size of talc at various level of specific kinetic energy

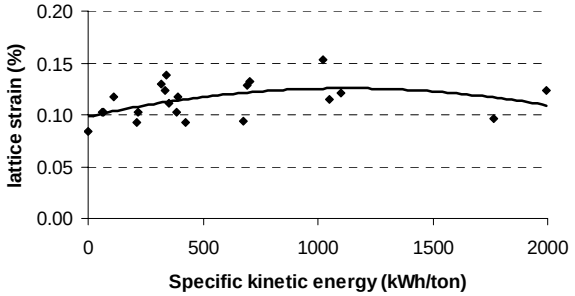

Figure 6. Lattice strain of talc at various level of specific kinetic energy

Figure 7 shows the summary of typical characteristics of ground talc at various levels of energy input and classifier rotational speed. These diagrams supported the idea that fine grinding process in jet mill induced mechanochemical effect besides size reduction and the breakage mechanism had an effect on the particle size and shape characteristics.

The results also showed that finer particles were obtained when talc were ground at low specific kinetic energy and classifier rotational speed which indicated that abrasion grinding mechanism producing finer particles, whilst coarser particles were obtained at high specific kinetic energy and classifier rotational speed.

High degree mechanochemical effect were induced on talc when it was ground at higher specific kinetic energy and classifier rotational speed which indicated destructive breakage mechanism had a pronounced effect on mechanochemical effect. Talc undergone delamination of nanosheets when it was ground at low specific kinetic energy with high classifier rotational speed. It exhibited angular and irregular particle shape at other operational parameters. Product in the medium level feed rate and grinding pressure exhibited the characteristics in between the low and high feed rate and grinding pressure respectively.

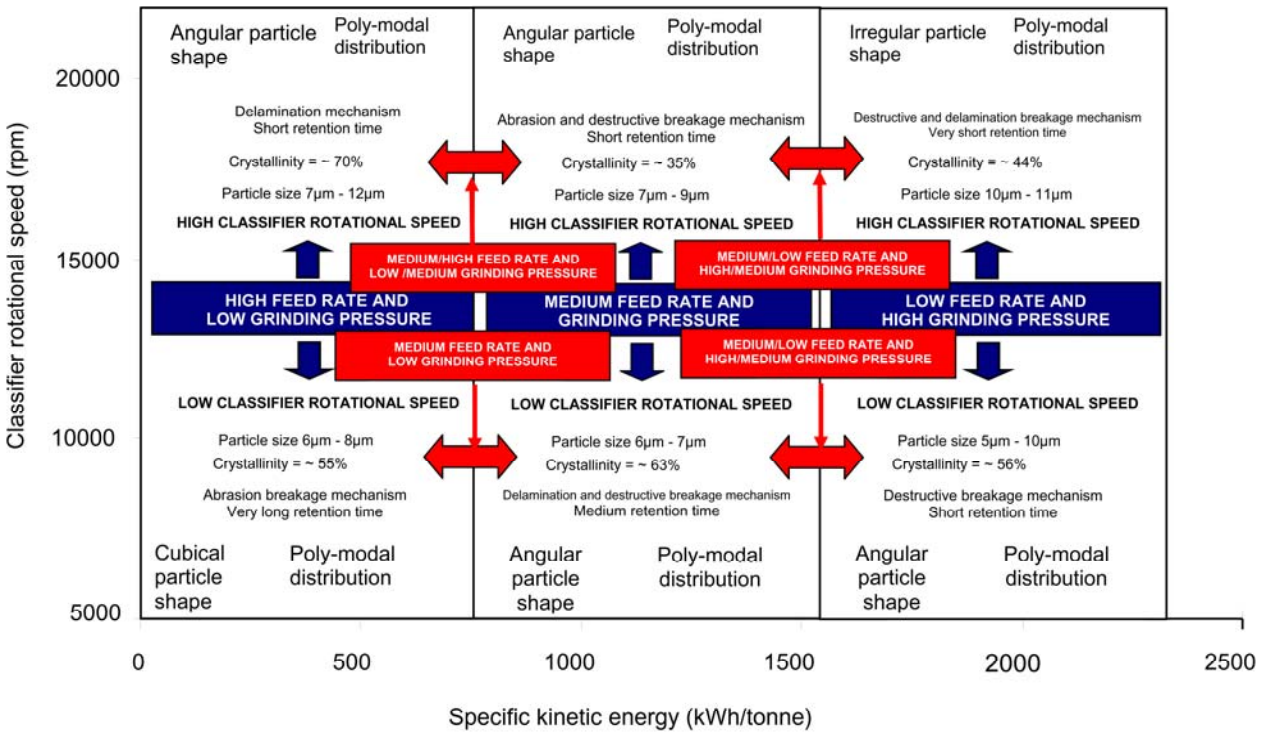

Figure 7. Summary of typical characteristics of ground talc at various levels of energy input and classifier rotational speed

Conclusions

The specific energy consumption exhibited transition value at 1000 kWh/ton for talc. These values indicated that further energy increase would be wasted as it was not effective for particle breakage. The mineralogical characteristics also played an important role in determining the optimum specific energy consumption. Furthermore, in terms of mechanochemical effect, the degree of crystallinity decreased as the specific kinetic energy increased although in this jet mill the grinding process was influenced by other parameters such as classifier rotational speed, holdup condition and grinding chamber pressure which was not taken into consideration during the calculation of specific kinetic energy.

Acknowledgement

The authors wish to gratefully acknowledge Universiti Sains Malaysia and Ministry of Higher Education, Malaysia for granting the research fund under Fundamental Research Grant (Project no.203/PBahan/6071123) for this research project.

References

1. P.J. Sanchez-Soto, A. Wiewiora, M.A. Aviles, A. Justo, L.A. Perez-Maqueda, J.L. Perez-Rodriguez, P. Bylina, Talc from Puebla de Lillo, Spain. II. Effect of dry grinding on particle size and shape. *Appl. Clay Sci.* 12 (1997) 297-312.
2. K. Terada, E. Yonemochi, Physicochemical properties and surface free energy of ground talc, *Solid State Ion.* 172 (2004) 459–462.
3. L. Godet-Morand, A. Chamayou, J. Dodds, Talc grinding in an oppose air jet mill: start-up, product quality and production rate optimisation. *Powder Tech.,* 128 (2002) 306-313
4. M. Benz, H. Herold, B. Ulfik, Performance of a fluidized bed jet mill as a function of operating parameters. *Int. J. of Miner. Process.,* 44-45 (1996) 507-519.
5. S. Molina-Boisseau, N. Le Bolay, M.N. Pons, Fragmentation mechanism of poly(vinyl acetate) particles during reduction in vibrated bead mill. *Powder Tech.,* 123 (2002) 282-291.
6. N. Midoux, P. Hosek, L. Pailleres, J.R. Authelin, Micronozation of pharmaceutical substances in a spiral jet mill. *Powder Tech.,* 104 (1999) 113-120.
7. H. Berthiaux, J. Dodds, Modelling fine grinding in a fluidized bed opposed jet mill. Part 1: Batch grinding kinetics. *Powder Tech*., 106 (1999) 78-87.
8. M. Mebtoul, J.F. Large, P. Guigon, High velocity impact of particles on a target – an experimantal study. *Inter. J. of Miner. Process*. 44-45 (1996) 77-91.
9. K.S. Venkataraman, K.S. Narayanan, Energetics of collision between grinding media in ball mills and mechanochemical effects. *Powder Tech.* 93 (1998) 190-201.

10. M.I. Al-Wakeel, Effect of mechanical treatment on the mineralogical constituents of Abu-Tartour phosphate ore, Egypt. *Int. J. of Miner. Process.,* 75 (2005) 101-112.
11. E.F. Aglietti, J.M. Porto Lopez, E. Pereira,. Mechanochemical effects in kaolinite grinding. II. Structural Aspects. *Int. J. of Miner. Process.* 16 (1986) 135-46.
12. Y. Kanno, Properties of SiC, Si_3N4 and SiO_2 ceramic powders produced by vibration ball milling. *Powder Tech.,* 44 (1985) 93–97.
13. S. Begin-Colin, T. Girot, A. Mocellin, G. Le Caer, Kinetics of formation of nano crystalline TiO_2 II by high energy ball milling of anatase TiO_2. *Nanostruct. Mater.* 12 (1999) 195-198.
14. H. Hu, Q. Chen, Z. Yin, P. Zhang, Thermal behaviour of mechanically activated pyrites by thermogravimetry (TG). *Thermochem. Acta.,* 398 (2003) 233-240.
15. J.C. Benezet, A. Benhassainne, Grinding and pozzolanic reactivity of quartz powders. *Powder Tech.,* 105 (1999) 167-171
16. A.Z. Juhasz, L. Opoczky, *Mechanical activation of minerals by grinding: Pulverizing and morphology of particles.* Ellis Horwood Limited. Chichester, 1990.
17. O. Lecoq, N. Chouteau, M. Mebtoul, J.F. Large, P. Guigon, Fragmantation by high velocity impact on a atrget: a material grindability test. *Powder Tech.,* 133. (2003) 113-124.
18. M. Nakach, J.R. Authelin, A. Chamayou, J. Dodds, Comparison of various milling technologies for grinding pharmaceutical powders. *Inter. J. of Miner. Process.,* 74S (2004) 173-S181.
19. P. Pourghahramani, E. Forssberg, Microstructure characterization of mechanically activated hematite using XRD line broadening. *Inter. J. of Miner. Process.* 79 (2006) 106–109.